Tetrahedron 64 (2008) 8476–8483

Contents lists available at ScienceDirect

Tetrahedron

journal homepage: www.elsevier.com/locate/tet

Electrospinning nanosuspensions loaded with passivated Au nanoparticles

Christopher A.E. Hamlett [a], Suwan N. Jayasinghe [b], Jon A. Preece [a,*]

[a] School of Chemistry, University of Birmingham, Edgbaston, Birmingham B15 2TT, United Kingdom
[b] Department of Mechanical Engineering, University College London, Torrington Place, London WC1E 7JE, United Kingdom

ARTICLE INFO

Article history:
Received 14 March 2008
Received in revised form 24 May 2008
Accepted 30 May 2008
Available online 5 June 2008

Keywords:
Au nanoparticles
Electrospinning
Composite fibres
Polyethylene oxide (PEO)

ABSTRACT

Aqueous polyethylene oxide (PEO) solutions (2 MDa, 2–5 wt %) with or without citrate passivated Au nanoparticles (5.7×10^{-7} wt %) have been electrospun, producing fibres with diameters from 290 μm to 55 nm. The incorporation of nanoparticles suppresses the diameter of the fibres and increases the degree of crystallinity. Such nanocomposite fibres are of interest as self-assembled templates for bottom-up fabrication methodologies.

1. Introduction

Electrospinning is an electrical, jet-based method of fabricating fibres based on the electrostatic repulsion of charges on the surface of a solution.[1–6] In comparison to conventional fibre processing methodologies, such as fibre drawing[7] and rotating disc[8,9] techniques, electrospinning has been shown to produce much finer fibres.[2] Electrospinning has been shown to routinely produce fibres of a wide variety of materials, from polymers[10,11] to ceramics,[12,13] in the sub-micron regime, and has even been used to process living cells.[14] Polymeric composite fibres[15] have also been fabricated by the electrospinning of polymeric solutions containing a wide variety of inclusions such as nanoparticles[16–20] and nanotubes.[19–21] The formation of composite nanofibres has been studied with a view for applications such as catalysis,[22,23] electronics,[24,25] drug delivery[6] and scaffolds for tissue engineering.[26–28] Electrospinning has also been shown to fabricate a range of fibre morphologies such as porous fibres[29] and non-woven mats[30] consisting of arrays of aligned fibres.[31,32] From an industrial viewpoint, electrospinning is a very attractive technique as it has been shown that electrospinning, using needle arrays, can be used to fabricate several square metres of non-woven mats of nanofibres.[30] Therefore, electrospinning can be used for high-throughput polymer processing.

Several groups[16–18] have previously studied the direct electrospinning of composite fibres containing Au nanoparticles. However, the previous studies on composite electrospun fibres containing Au nanoparticles have not reported the viscosities of the polymeric composite solutions.[16–18] Therefore, the work presented in this paper investigates the morphology of fibres electrospun from high viscosity aqueous solutions of composite polyethylene oxide (PEO)/negatively charged[33] citrate passivated Au nanoparticles. High viscosity PEO composite solutions reported are of the order of 8900 mPa s.[34] The effect of the viscosity of the PEO solutions and the inclusion of Au nanoparticles within the composite polymeric solutions on the size of the electrospun fibres is studied. The morphology of the electrospun fibres is investigated by both optical microscopy and atomic force microscopy (AFM), and the crystallinity of the fibres will be studied using AFM and differential scanning calorimetry (DSC). Transmission electron microscopy (TEM) is used to investigate the arrangement of the nanoparticles within the fibres.

2. Results and discussion

2.1. Nanosuspension batch preparation and stability

Citrate passivated Au nanoparticles were synthesised using the Frens method[35] and characterised using UV–vis spectroscopy and TEM. The UV–vis spectrum (Fig. 1a, also see Supplementary data) shows that the citrate passivated Au nanoparticle solution exhibits the characteristic surface plasmon band of discrete Au nanoparticles at ~524 nm.[33]

A histogram showing the size distribution of the citrate passivated Au nanoparticles (Fig. 1b) was obtained from TEM images (an example of which is shown in Fig. 1c) revealing an average particle diameter of 7.8 nm±0.1 nm (based on 1069 particles). An

* Corresponding author. Tel.: +44 (0) 121 414 3528; fax: +44 (0) 121 414 4403.
E-mail address: j.a.preece@bham.ac.uk (J.A. Preece).

0040-4020/$ – see front matter © 2008 Elsevier Ltd. All rights reserved.
doi:10.1016/j.tet.2008.05.134

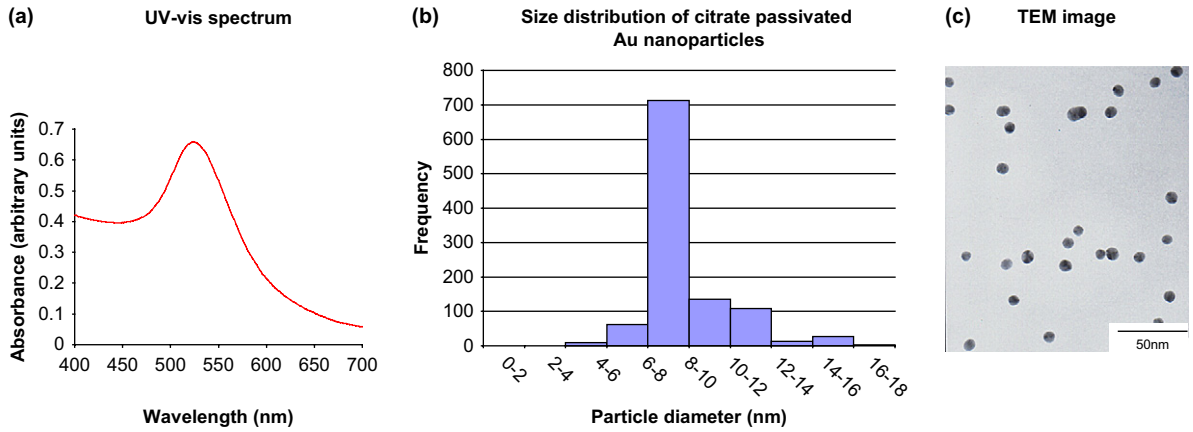

Figure 1. (a) UV–vis spectra of citrate passivated Au nanoparticles and (b) a histogram showing the size distribution of citrate passivated Au nanoparticles. (c) A representative TEM image of citrate passivated Au nanoparticles. The mean particle diameter is 7.8±0.1 nm.

estimation of the colloidal concentration in the suspension, 1.2×10^{9} Au particles ml^{-1}, was deduced, from TEM images.

2.2. Characterisation of fibres electrospun from PEO solutions

Fibres were electrospun from aqueous solution containing 2, 3, 4 and 5 wt% of PEO with and without Au nanoparticles (5.6×10^{-7} wt%). Optical, AFM and TEM micrographs of the fibres are shown in Figure 2 revealing that the fibres are produced across the range of diameters from 290 μm to 55 nm.

Optical microscopy and AFM were used to measure the widths of fibres electrospun from 2, 3, 4 and 5 wt% aqueous solutions of PEO and PEO/Au nanoparticle composite. Histograms depicting the global distribution of fibre widths were determined by optical microscopy and AFM (Fig. 3). Histograms of fibre widths determined solely by AFM are shown in Figure 4. Histograms of the global fibre width distribution exhibit a bimodal distribution for fibres electrospun from aqueous PEO solutions (Fig. 3a), with the larger diameter decreasing with increasing PEO concentration (106 to 76 μm). However, inclusion of citrate passivated Au nanoparticles in the PEO solution results in the distribution changing from bimodal to a unimodal distribution (Fig. 3b), with the larger fibre diameters being suppressed. Histograms obtained from AFM data reveal broad distributions of fibre diameters on the sub 2 μm length scale (Fig. 4) with the inclusion of Au nanoparticles appearing to have little effect on the distribution of fibre diameters.

In order to investigate the loading of the Au nanoparticles within the electrospun nanofibres, TEM images (Fig. 5) were obtained of fibres electrospun directly onto TEM Cu slot grids. TEM images (Fig. 5a and b) show nanoparticulate clusters, which are present in both the threads and the beads. Such beaded fibres form as a result of surface tension forces causing the PEO solution to build up at the needle tip.[28] Once the repulsive forces of the charged solution surface overcome the surface tension forces the jetting occurs from the bead, and it detaches from the needle tip forming a fibre with a bead and thread morphology.[30] However, the nanoparticles are more concentrated in the beads ($\sim4.3\times10^{13}$ particles ml^{-1}) than in the threads ($\sim3.5\times10^{12}$ particles ml^{-1}). This observation may be related to the differences in surface tensions between bead formation and non-bead formation, resulting

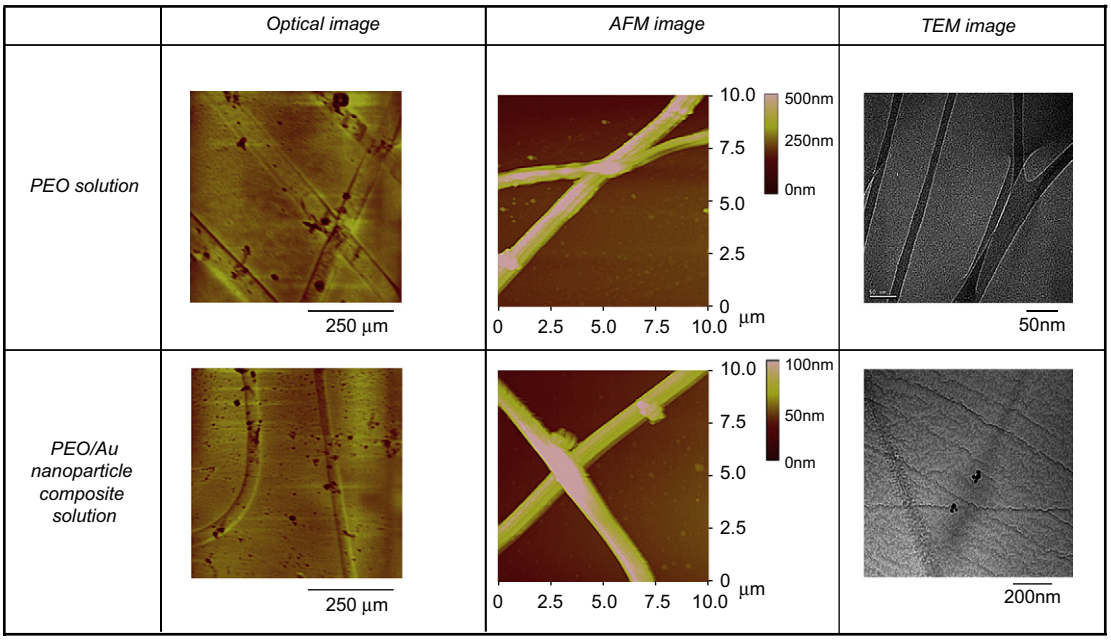

Figure 2. Optical, AFM and TEM images of fibres electrospun from either PEO solution or PEO/Au nanoparticle composite solution.

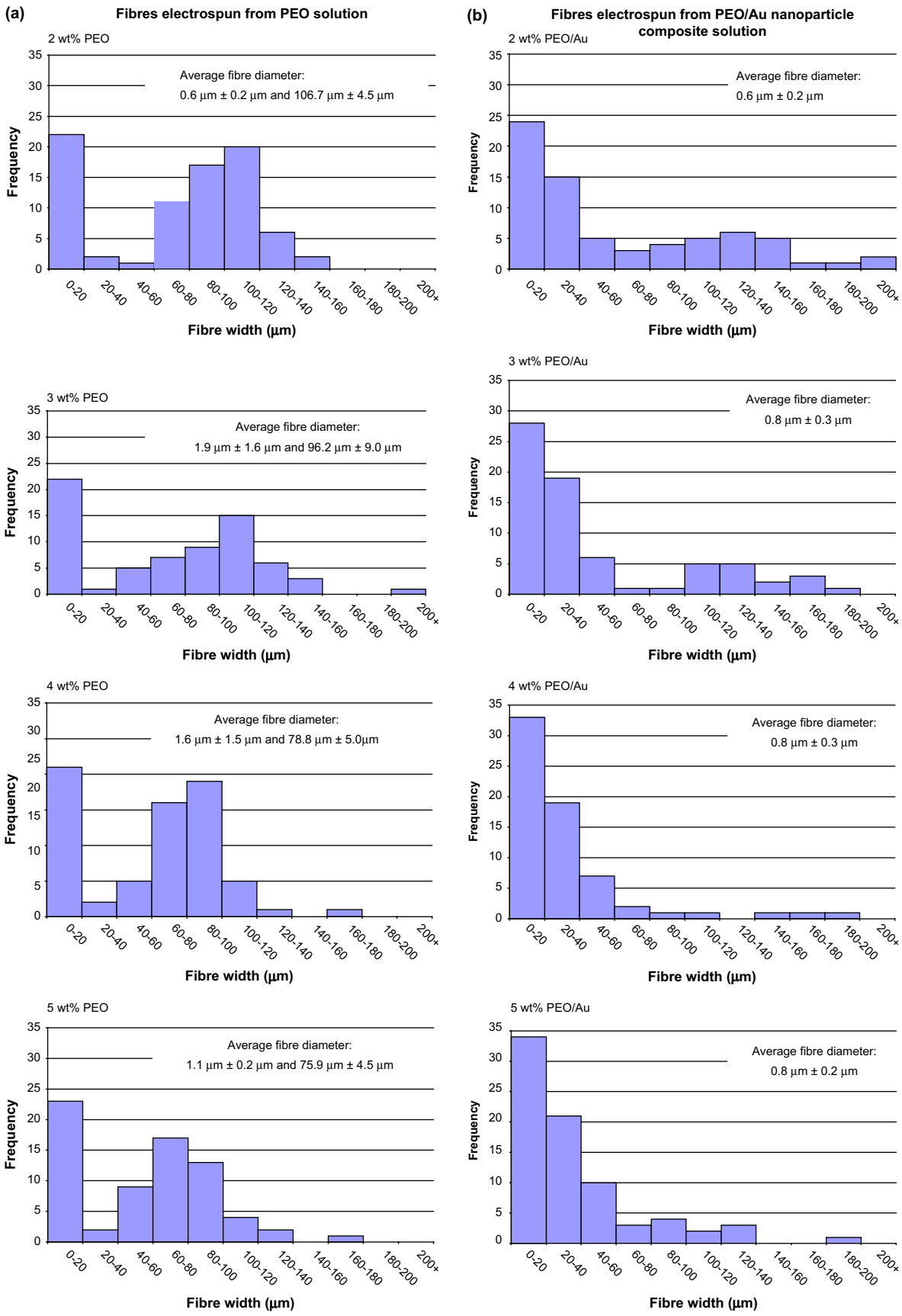

Figure 3. Histograms showing the global distribution of widths of fibres electrospun from aqueous solutions of PEO and PEO/Au nanoparticles as calculated from both AFM and optical micrographs. Average fibre widths for each system are shown in brackets.

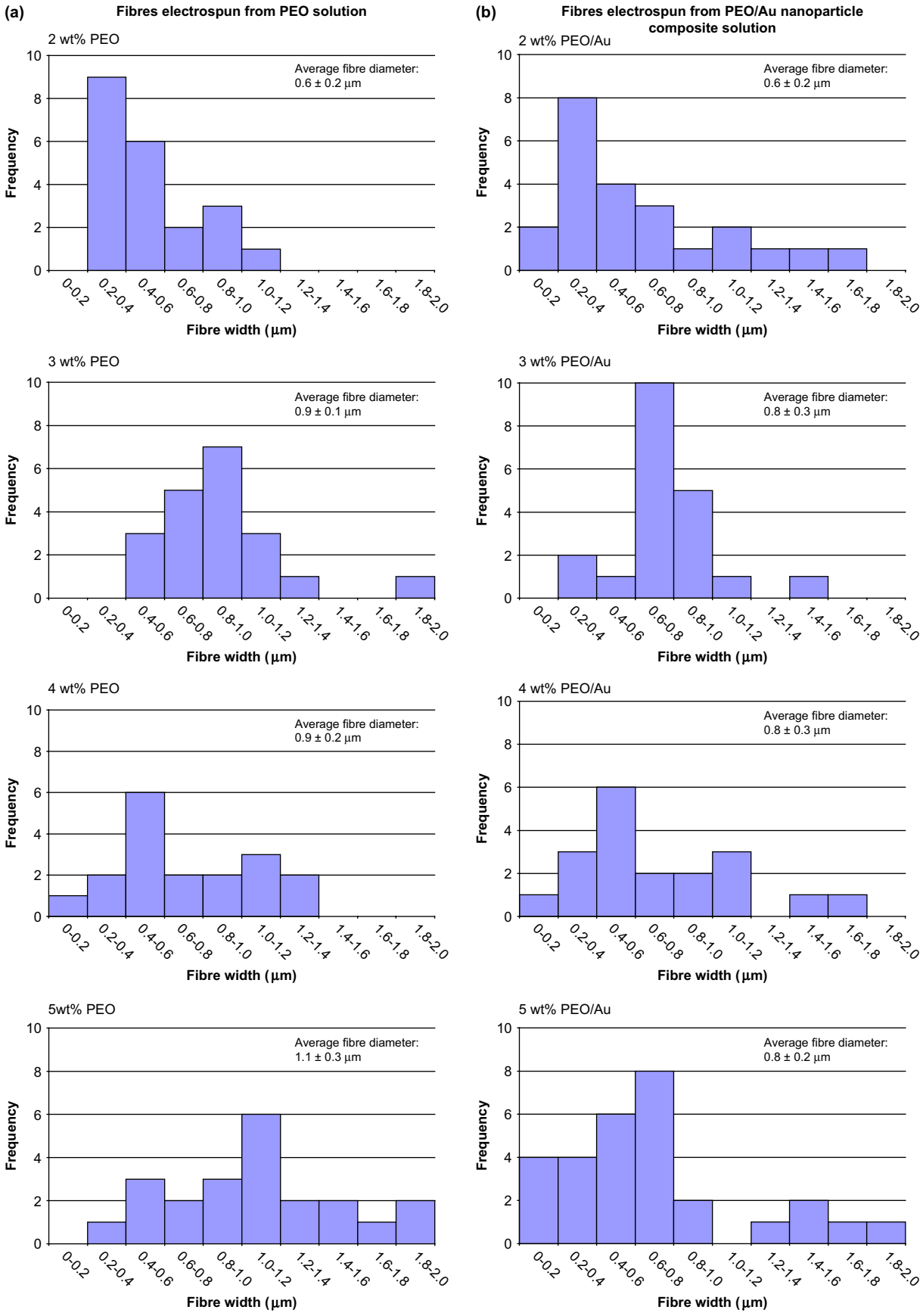

Figure 4. Histograms showing the widths of fibres electrospun from aqueous solutions of PEO and PEO/Au nanoparticles as calculated from AFM images. Average fibre widths for each system are shown in brackets.

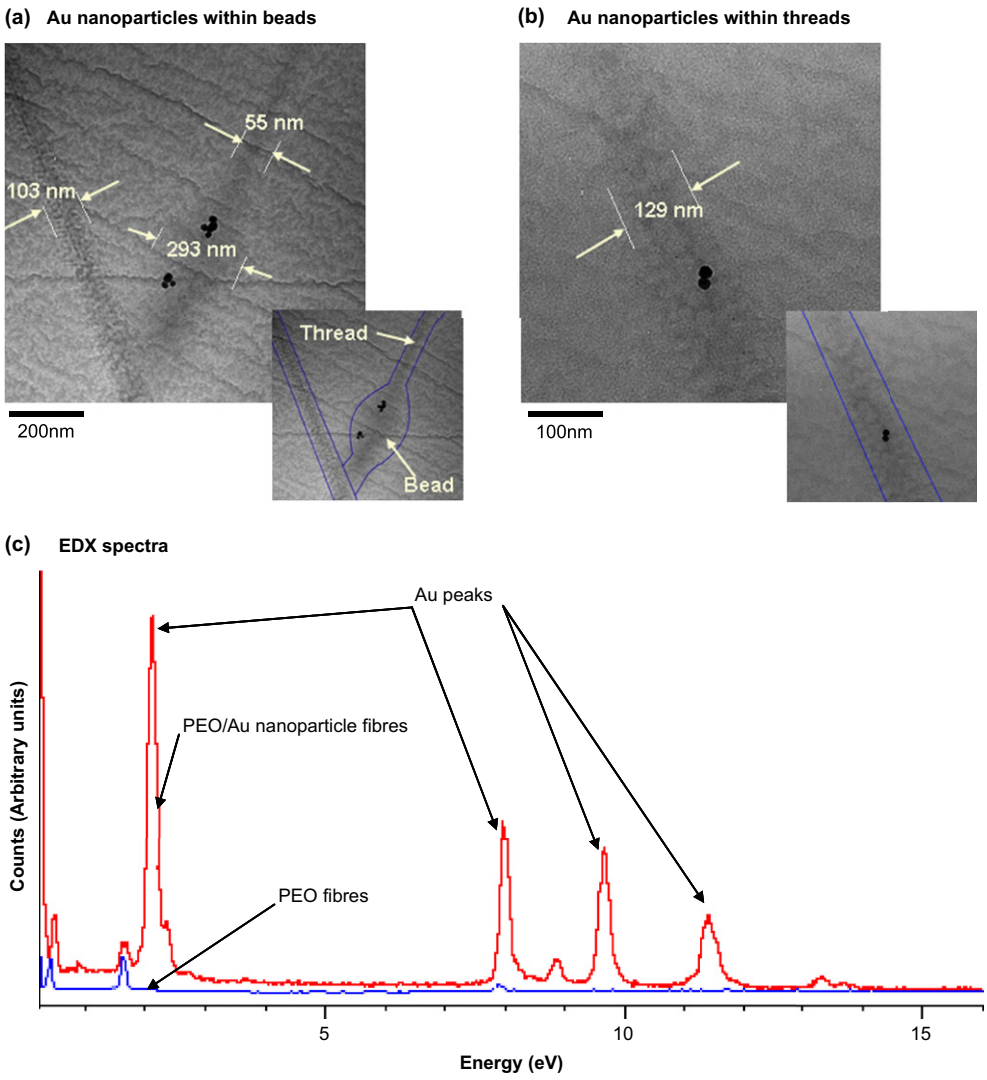

Figure 5. TEM images showing (a) the presence of Au nanoparticles in 'beads' and (b) the presence of Au nanoparticles within 'threads' (the insets for both (a) and (b) show outlines of the fibres for clarity). (c) EDX spectra of fibres electrospun from solutions of 5 wt % PEO either with or without the presence of Au nanoparticles.

in the increased particle density in the beads. Previous studies of the distribution of Au nanoparticles within electrospun PEO/Au composite fibres by Kim et al.[16] reveal chain-like arrays of Au nanoparticles. However, the Au nanoparticles studied by Kim et al.[16] were uncharged as they were passivated by dodecanethiol as opposed to the citrate passivated Au nanoparticles (negatively charged) used in the study presented in this paper. Presumably the electrostatic repulsion of the negatively charged Au nanoparticles may hinder the formation of one dimensional chain-like arrays.

EDX spectra (Fig. 5c) confirmed both the absence and the presence of elemental Au within fibres electrospun from PEO solutions and PEO/Au nanoparticle solutions, respectively. This observation is rationalised by the evolution of Au peaks in the EDX spectrum upon inclusion of Au nanoparticles in the electrospinning solution (Fig. 5c).

It is noteworthy that both the concentration of the PEO and the inclusion of nanoparticles in the electrospinning solution had an effect on the crystallinity of the generated fibres. Areas of crystallinity were observed in the AFM phase images (Fig. 6b) as lamellar structures,[16] which are representative of 'shish-kebab' arrangements of crystalline PEO that cannot be seen in AFM height images (Fig. 6a). AFM phase imaging measures the phase lag of the cantilever oscillation during AFM imaging, which is very sensitive to adhesion between the tip and the sample.[36] Therefore, phase imaging can be used to differentiate between amorphous and crystalline regions of a semi-crystalline polymer, which are indistinguishable in AFM height imaging.[36] The formation of crystalline regions of the PEO fibres may be due to flow-induced crystallisation[37] whereby the PEO chains are aligned parallel to the flow direction due to the whipping instability of the electrospinning jet.[38] DSC analysis was used to determine the enthalpy of fusion (ΔH_f) of fibres spun from each solution and this information was used to calculate the % crystallinity of electrospun fibres by comparing the measured ΔH_f of the electrospun fibres to that of 100% crystalline PEO. Such a method has previously been used to determine the degree of crystallinity of electrospun fibres.[16] ΔH_f for each wt % PEO solution (Table 1) was compared to ΔH_f of 100% crystalline PEO, which is 205 J g^{-1},[39] in order to determine the degree of crystallinity of the fibres (Table 1 and Fig. 6c).

Table 1 shows that both ΔH_f and % crystallinity increase as the wt % PEO of the solutions is increased. The % crystallinity also increases upon the introduction of Au nanoparticles into the solution (Fig. 6c). The increase of crystallinity, upon the inclusion of Au nanoparticles, may occur due to one, or both, of the two reasons. One reason may be due to the nanoparticles acting as heterogeneous nucleation sites for polymer crystallisation as previously

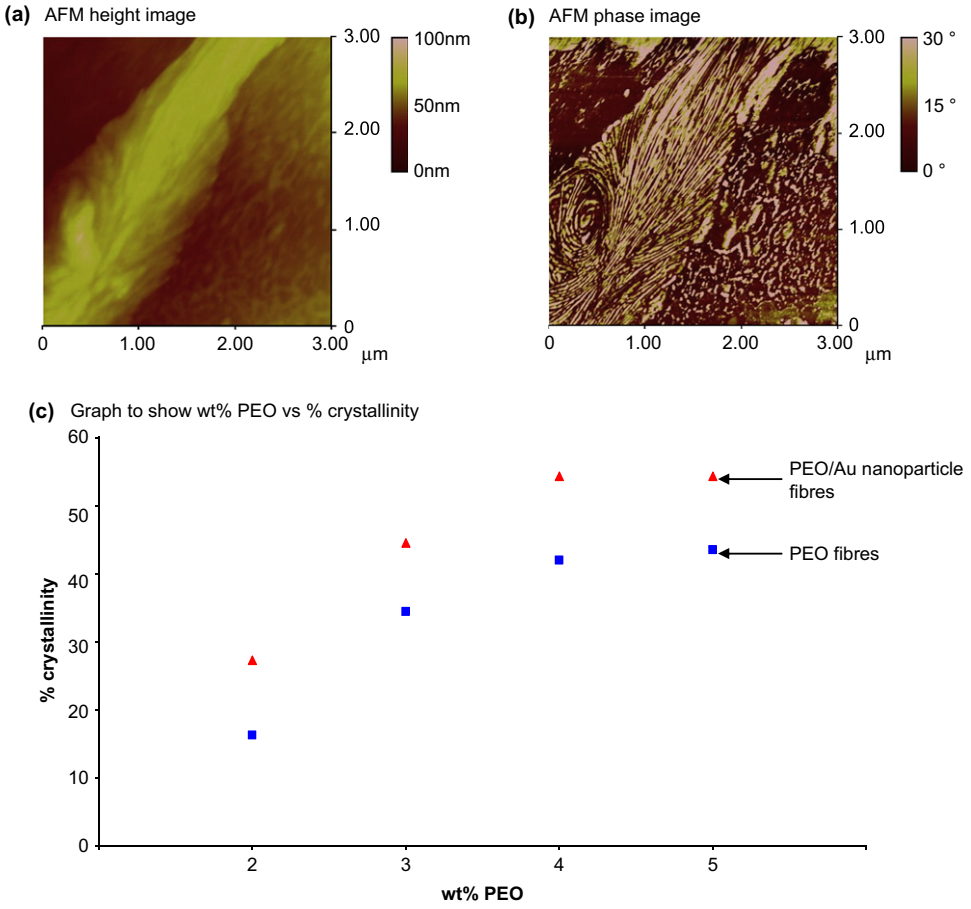

Figure 6. AFM (a) height and (b) phase images of a fibre electrospun from 4 wt % PEO solution in UHQ H_2O. (c) Graph showing the % crystallinity of fibres electrospun from aqueous PEO solutions either with or without the presence of citrate passivated Au nanoparticles.

shown.[40,41] Another explanation for the inclusion of Au nanoparticles resulting in increased crystallinity may be that the particles inhibit the relaxation of PEO molecules after the initial flow-induced crystallisation.

3. Conclusions

These studies demonstrate the ability to directly form composite fibres from highly viscous PEO/Au nanoparticle solutions. Citrate passivated Au nanoparticles were doped into PEO solutions and electrospun, producing fibres with diameters in the range of 290 µm to 55 nm. Fibres without the nanoparticles produced a bimodal distribution of fibre diameters with the larger diameter decreasing with increasing PEO concentration (106 to 76 µm), whereas the fibres containing the Au nanoparticles suppressed the formation of the larger diameter fibres. TEM analysis of the smallest fibres reveals that the Au nanoparticle distribution within the fibres is more concentrated in the 'beaded' areas of the fibres. This increase may be due to surface tension effects. Interestingly, introduction of the Au nanoparticles increased the degree of crystallinity of all the PEO fibres, which may be due to the nanoparticles acting as either nucleation sites or pinning the crystalline PEO, which is formed due to flow-induced crystallisation during electrospinning.

Table 1
Viscosity of the electrospinning solutions, and the enthalpy of fusion and % crystallinity of the electrospun fibres

PEO solution (wt %)	Viscosity (mPa s)		ΔH_f (J g^{-1}) [onset temperature (°C)]	% Crystallinity	ΔH_f (J g^{-1}) [onset temperature (°C)]	% Crystallinity[b]	Δ% Crystallinity[c]
	Aqueous PEO solution	Aqueous PEO/Au nanoparticle solution[a]	Without nanoparticles		With Au nanoparticles		
2	1921	1894	33.51 [56.1]	16.35	55.88 [54.9]	27.26	67
3	5132	4966	70.66 [53.9]	34.47	91.20 [53.0]	44.49	29
4	7328	7210	86.02 [52.0]	41.96	111.29 [53.9]	54.29	29
5	10,230	9534	89.23 [53.7]	43.53	111.37 [52.6]	54.32	24

[a] Loading of Au nanoparticles in all PEO/Au electrospinning solutions was 5.6×10^{-7} wt %.
[b] % Crystallinity is calculated by dividing ΔH_f (measured) by ΔH_f (from the literature for 100% crystalline PEO then multiplying by 100). The literature value for 100% crystalline PEO is 205 J g^{-1}.[39]
[c] Δ% Crystallinity between fibres without Au nanoparticles and those with Au nanoparticle inclusions.

The inclusion of Au nanoparticles within the fibres could allow for the fabrication of nanoscale Au templates after patterned fabrication of the composite fibres and subsequent removal of the PEO matrix. Such templates could be used for the bottom-up fabrication of nanostructures in conjunction with alkanethiol self-assembled monolayers (SAMs).

4. Experimental

4.1. Materials

All chemicals were purchased from Aldrich unless otherwise specified.

4.2. Gold nanoparticle solution

4.2.1. Citrate passivated gold nanoparticle preparation

Aqueous solutions of citrate passivated Au nanoparticles were prepared by the method described by Frens.[35] A solution of chloroauric acid (0.01 g, 2.5 mmol in UHQ water) was heated under reflux for 2 h. Sodium citrate tribasic dihydrate (0.023 g, 0.15 mol) was added to the refluxing chloroauric acid solution and heating continued until there was no further colour change (colourless to red). The solution was allowed to cool to room temperature, centrifuged and the supernatant, containing the nanoparticles, was retained.

4.2.2. UV–vis spectroscopy

UV–vis spectra of the citrate passivated Au nanoparticle solutions were obtained using a Hewlett–Packard 8452A spectrometer operated at wavelengths between 350 and 850 nm with a 2 nm band width at 240 nm min^{-1}.

4.2.3. TEM

TEM specimens of citrate passivated Au nanoparticles were prepared by placing a drop of aqueous citrate passivated Au nanoparticle solution ($\sim$3 ml) on a Formvar coated Cu TEM grid (Agar) and allowed to air-dry. TEM characterisation of citrate passivated Au nanoparticles was performed using a JEOL 1200ex TEM operated at 80 kV.

4.3. Electrospinning

4.3.1. Preparation of solutions for electrospinning

Polyethylene oxide (PEO) solutions were prepared by adding powdered PEO (2 MDa) to either UHQ H_2O (resistivity=18 MΩ cm) or an aqueous solution of citrate passivated Au nanoparticles. The powdered PEO was added, over a period of 10 min, to either the UHQ H_2O or the nanoparticle solution under vigorous stirring in a 100 ml glass Duran flask and stirred for further 24 h.

4.3.2. Viscosity measurements

In these experiments, the viscosity of all solutions was independently measured each using a Visco-Easy rotational viscometer as previously described.[42] Several repeated measurements were made for fresh aliquots of the respective solution. Table 1 summarises the viscosity data.

4.3.3. Electrospinning process

Electrospinning was carried out with a standard spinning set-up as previously described[42] with a wide operational parametric space of $\sim$1 to 30 kV and $\sim10^{-8}$ to 10^{-15} $m^3\,s^{-1}$ for the applied voltage and flow rate, respectively. It is well known that in electrospinning studies there are three important parameters, which need to be controlled. These are namely (i) the applied voltage to the needle with respect to the collector or ground element, (ii) the flow rate and its consistency to the needle and (iii) the solution properties such as the viscosity and electrical conductivity. During these studies, we traversed a wide operational range and found that all our formulated solutions threaded with stability at selected parametric conditions of $\sim$12 kV and $\sim10^{-9}$ $m^3\,s^{-1}$ for the applied voltage and flow rate, respectively. The solutions were electrospun onto either glass microscopic slides (for AFM and DSC analyses) or onto TEM grids.

4.3.4. AFM and optical microscopies

AFM images were obtained using either a Nanoscope 3100 Dimension AFM (Veeco) or a PicoScan AFM (Molecular Imaging) and these images were analysed using either Nanoscope III software (version 5.12r3) or PicoScan 5 software, respectively. AFM images were obtained in tapping mode with the use of an etched silicon tip (Veeco model: RTESP). The AFM tip was engaged with the surface and the images were obtained in tapping mode at a frequency of 1 Hz and the images were made up of 512 lines with 512 samples per line. Optical micrographs were obtained using the optical system of the Nanoscope 3100 Dimension AFM.

4.3.5. TEM

Electrospun fibres were prepared for characterisation by TEM by electrospinning the fibres directly onto copper slot TEM grids (Agar Scientific). TEM characterisation of the electrospun fibres was carried out using a Technai F20 FEG TEM (Philips) operated at 200 kV.

4.3.6. EDX

EDX spectra were obtained in situ in the Technai F20 FEG TEM and analysed by using ISIS 300 EDX software (Oxford Instruments).

4.3.7. DSC

DSC measurements were recorded by placing $\sim$1 mg of PEO or PEO/Au nanoparticle fibres into an Al pan onto which a lid was placed, crimped closed and placed into a differential scanning calorimeter (Perkins Elmer Pyris with Pyris control software) along with an empty pan, which was used as a control. The pan was held at 25 °C for 1 min, then heated to 120 °C at 5 °C min^{-1} and then held at 120 °C for 1 min before being cooled to 25 °C at -5 °C min^{-1}.

Acknowledgements

This work was supported by the Engineering and Physical Sciences Research Council (CAEH and JAP) and the EU NANO3D project (Grant number NMP-CT-2005-104006). SNJ gratefully thanks the Royal Society of UK for financially supporting this work.

Supplementary data

Supplementary data associated with this article can be found in the online version, at doi:10.1016/j.tet.2008.05.134.

References and notes

1. Li, D.; Xia, Y. *Adv. Mater.* **2004**, *16*, 1151–1170.
2. Rutledge, G. C.; Fridrikh, S. V. *Adv. Drug Delivery Rev.* **2007**, *59*, 1384–1391.
3. Venugopal, J.; Vadgama, P.; Sampath Kumar, T. S.; Ramakrishna, S. *Nanotechnol.* **2007**, *18*, 055101 (8p).
4. Subbiah, T.; Bhat, G. S.; Tock, R. W.; Parameswaran, S.; Ramkumar, S. S. *J. Appl. Polym. Sci.* **2005**, *96*, 557–569.
5. Li, X. H.; Shao, C. L.; Liu, Y. C. *Langmuir* **2007**, *23*, 10920–10923.
6. Taepaiboon, P.; Rungsardthong, U.; Supaphol, P. *Nanotechnol.* **2006**, *17*, 2317–2329.
7. Ondarçuhu, T.; Joachim, C. *Europhys. Lett.* **1998**, *42*, 215–220.
8. Schultz, J. M.; Hsiao, B. S.; Samon, J. M. *Polymer* **2000**, *41*, 8887–8895.
9. Lopes, P. E.; Ellison, M. S.; Pennington, W. T. *Plast. Rubber Compos.* **2006**, *35*, 294–300.
10. Pan, C.; Ge, L. Q.; Gu, Z. Z. *Compos. Sci. Technol.* **2007**, *67*, 3271–3277.

11. Dersch, R.; Steinhart, M.; Boudriot, U.; Greiner, A.; Wendorff, J. H. *Polym. Adv. Technol.* **2005**, *16*, 276–282.
12. Sigmund, W.; Yuh, J.; Park, H.; Maneeratana, V.; Pyrgiotakis, G.; Daga, A.; Taylor, J.; Nino, J. C. *J. Am. Ceram. Soc.* **2006**, *89*, 395–407.
13. Li, D.; McCann, J. T.; Xia, Y.; Marquez, M. *J. Am. Ceram. Soc.* **2006**, *89*, 1861–1869.
14. Jayasinghe, S. N.; Irvine, S.; McEwan, J. R. *Nanomed.* **2007**, *2*, 555–567.
15. Sawicka, K. M.; Gouma, P. *J. Nanopart. Res.* **2006**, *8*, 769–781.
16. Kim, G. M.; Wutzler, A.; Radesch, H. J.; Michler, G. H.; Simon, P.; Sperling, R. A.; Parak, W. J. *Chem. Mater.* **2005**, *17*, 4949–4957.
17. Bai, J.; Li, Y.; Yang, S.; Du, J.; Wang, S.; Zheng, J.; Wang, Y.; Yang, Q.; Chen, X.; Jing, X. *Solid State Commun.* **2007**, *141*, 292–295.
18. Wang, Y.; Li, Y.; Sun, G.; Zhang, G.; Liu, H.; Du, J.; Yang, S.; Bai, J.; Yang, Q. *J. Appl. Polym. Sci.* **2007**, *105*, 3618–3622.
19. Salalha, W.; Dror, Y.; Khalfin, R. L.; Cohen, Y.; Yarin, A. L.; Zussman, E. *Langmuir* **2004**, *20*, 9852–9855.
20. Mathew, G.; Hong, J.; Rhee, J. M.; Lee, H. S.; Nah, C. *Polym. Test.* **2005**, *24*, 712–717.
21. Yang, B. X.; Shi, J. H.; Pramoda, K. P.; Goh, S. H. *Nanotechnol.* **2007**, *18*, 125606 (7pp).
22. Stasiak, M.; Struder, A.; Greiner, A.; Wendorff, J. H. *Chem.—Eur. J.* **2007**, *13*, 6150–6156.
23. Wang, Z. G.; Ke, B. B.; Xu, Z. K. *Biotechnol. Bioeng.* **2007**, *97*, 708–720.
24. Miezawska, A. J.; Jalilian, R.; Sumanasekera, G. U.; Zamborini, F. P. *Small* **2007**, *3*, 722–756.
25. Jin, M.; Zhang, X.; Nishimoto, S.; Liu, Z.; Tryk, D. A.; Murakami, T.; Fujishima, A. *Nanotechnol.* **2007**, *18*, 075605 (7pp).
26. Li, W. J.; Mauck, R. L.; Cooper, J. A.; Yuan, X.; Tuan, R. S. *J. Biomech.* **2007**, *40*, 1686–1693.
27. Jiang, H.; Zhao, P.; Zhu, K. *Macromol. Biosci.* **2007**, *7*, 517–525.
28. Lannutti, J.; Reneker, D.; Ma, T.; Tomasko, D.; Farson, D. *Mater. Sci. Eng., C* **2007**, *27*, 504–509.
29. Dayal, P.; Liu, J.; Kumar, J. S.; Kyu, T. *Macromolecules* **2007**, *40*, 7689–7694.
30. Ramakrishna, S.; Fujihara, K.; Teo, W.-E.; Lim, T.-C.; Ma, Z. *An Introduction to Electrospinning and Nanofibres*; World Scientific: London, 2005.
31. Kameoka, J.; Orth, R.; Yang, Y.; Czaplewski, D.; Mathers, R.; Coates, G. W.; Craighead, H. G. *Nanotechnol.* **2003**, *14*, 1124–1129.
32. Gu, B. K.; Sohn, K.; Kim, S. J.; Kim, S. I. *J. Nanosci. Nanotech.* **2007**, *7*, 4202–4205.
33. Diegoli, S.; Mendes, P. M.; Baguley, E. R.; Leigh, S. J.; Iqbal, P.; Garcia Diaz, Y. R.; Begum, S.; Critchley, K.; Hammond, G. D.; Evans, S. D.; Attwood, D.; Jones, I. P.; Preece, J. A. *J. Exp. Nanosci.* **2006**, *1*, 333–353.
34. Liu, Y.; Chen, J.; Miskoska, V.; Wallace, G. G. *React. Funct. Polym.* **2007**, *67*, 461–467.
35. Frens, G. *Nat. Phys. Sci.* **1973**, *241*, 20–22.
36. Babcock, K. L.; Prater, C. B. *Digital Instruments—SPM Application Notes (AN11)*; Veeco Instruments: Santa Barbara, CA, 1995.
37. Zussman, E.; Rittel, D.; Yarin, A. L. *Appl. Phys. Lett.* **2003**, *82*, 3958–3960.
38. Lim, C. T.; Tan, E. P. S.; Ng, S. *IEEE Trans. Dielectr. Electr. Insul.* **2008**, *92*, 141908(3p).
39. Yang, Y.; Jia, Z.; Li, Q.; Guan, Z. *IEEE Trans. Dielectr. Electr. Insul.* **2006**, *13*, 580–585.
40. Saujanya, C.; Radhakrishnan, S. *Polymer* **2001**, *42*, 6723–6731.
41. Elias, H.-G. *An Introduction to Polymer Science*; VCH: Weinheim, 1997.
42. Wang, D. Z.; Jayasinghe, S. N.; Edirisinghe, M. J.; Luklinska, Z. B. *J. Nanopart. Res.* **2007**, *9*, 825–831.